



More enhanced non-growing season methane exchanges under warming on the Qinghai-Tibetan Plateau



Zhenhai Liu^{a,b,c}, Bin Chen^{a,c,*}, Shaoqiang Wang^{a,b,d,e,**}, Xiyan Xu^f, Huai Chen^{g,h}, Xinwei Liu^{g,h}, Jin-Sheng He^{i,j}, Jianbin Wangⁱ, Jinsong Wang^a, Jinghua Chen^a, Xiaobo Wang^a, Chen Zheng^{a,b}, Kai Zhu^{a,b}, Xueqing Wang^{a,b}

^a Key Laboratory of Ecosystem Network Observation and Modeling, Institute of Geographic Sciences and Natural Resources Research, Chinese Academy of Sciences, Beijing 100101, China

^b College of Resources and Environment, University of Chinese Academy of Sciences, Beijing 100049, China

^c Key Laboratory of Coupling Process and Effect of Natural Resources Elements, Beijing, 100055, China

^d Hubei Key Laboratory of Regional Ecology and Environmental Change, School of Geography and Information Engineering, China University of Geosciences, Wuhan 430078, China

^e Technology Innovation Center for Intelligent Monitoring and Spatial Regulation of Land Carbon Sequestrations, Ministry of Natural Resources, Wuhan 430078, China

^f Key Laboratory of Regional Climate-Environment for Temperate East Asia, Institute of Atmospheric Physics, Chinese Academy of Sciences, Beijing 100029, China

^g Key Laboratory of Mountain Ecological Restoration and Bioresource Utilization & Ecological Restoration Biodiversity Conservation Key Laboratory of Sichuan Province, Chengdu Institute of Biology, Chinese Academy of Sciences, Chengdu 610041, China

^h Zoige Peatland and Global Change Research Station, Chinese Academy of Sciences, Hongyuan 624400, China

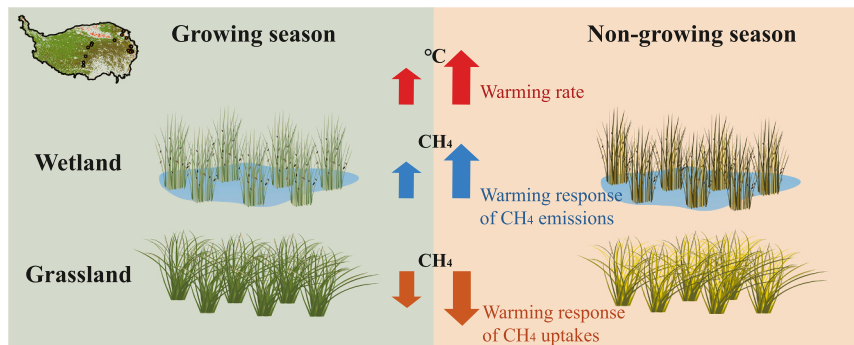
ⁱ State Key Laboratory of Herbage Improvement and Grassland Agro-ecosystems, College of Pastoral Agriculture Science and Technology, Lanzhou University, Lanzhou 730000, China

^j Department of Ecology, College of Urban and Environmental Sciences, and Key Laboratory for Earth Surface Processes of the Ministry of Education, Peking University, Beijing 100871, China

HIGHLIGHTS

- Warming promoted CH₄ emissions in wetlands and uptakes in grasslands on the QTP.
- CH₄ exchange has stronger response to warming in non-growing than growing season.
- The seasonality was analyzed using 9745 daily observations and four approaches.
- Asymmetrical seasonal warming and responses of CH₄ exchange regulate QTP CH₄ budget.

GRAPHICAL ABSTRACT



* Corresponding author.

** Correspondence to: S. Wang, Key Laboratory of Ecosystem Network Observation and Modeling, Institute of Geographic Sciences and Natural Resources Research, Chinese Academy of Sciences, Beijing 100101, China.

E-mail addresses: chenbin@igsnrr.ac.cn (B. Chen), sqwang@igsnrr.ac.cn (S. Wang).

ARTICLE INFO

Editor: Zhaozhong Feng

Keywords:

Methane exchange
The Qinghai-Tibetan Plateau
Temperature sensitivity
Seasonality
Data integration
Machine learning

ABSTRACT

Uncertainty in methane (CH_4) exchanges across wetlands and grasslands in the Qinghai-Tibetan Plateau (QTP) is projected to increase due to continuous permafrost degradation and asymmetrical seasonal warming. Temperature plays a vital role in regulating CH_4 exchange, yet the seasonal patterns of temperature dependencies for CH_4 fluxes over the wetlands and grasslands on the QTP remain poorly understood. Here, we demonstrated a stronger warming response of CH_4 exchanges during the non-growing season compared to the growing season on the QTP. Analyzing 9745 daily observations and employing four methods—regression fitting of temperature- CH_4 flux, temperature dependence calculations, field-based and model-based control experiments—we found that warming intensified CH_4 emissions in wetlands and uptakes in grasslands. Specifically, the average reaction intensity in the non-growing season surpasses that in the growing season by 1.89 and 4.80 times, respectively. This stronger warming response of CH_4 exchanges during the non-growing season significantly increases the regional CH_4 exchange on the QTP. Our research reveals that CH_4 exchanges in the QTP have a higher warming sensitivity in non-growing seasons, which meanwhile are dominated by a larger warming rate than the annual average. The combined effects of these two factors will significantly alter the CH_4 source/sink on the QTP. Neglecting these impacts would lead to inaccurate estimations of CH_4 source/sink over the QTP under climate warming.

1. Introduction

Methane (CH_4) has 28 times greater global warming potential than CO_2 over a century and it is the second most impactful greenhouse gas (Shindell et al., 2009; Zhang et al., 2023). Bottom-up estimates attribute about 50.65 % of the total global CH_4 sources to natural emissions and about 4.80 % of the total global CH_4 sinks to soil uptakes (Saunois et al., 2020). Numerous studies have indicated that climate warming can markedly affect terrestrial ecosystem CH_4 exchanges, producing positive or negative feedbacks on the rate of climate warming (Wang et al., 2022; Yvon-Durocher et al., 2014; Zona et al., 2016). Understanding the response of ecosystem CH_4 exchanges is therefore crucial for assessing and predicting biosphere-atmosphere feedback in a warming world. However, since most studies on the warming response of CH_4 exchanges have not explored the temporal variation (Bao et al., 2021; Chen et al., 2021b; Yvon-Durocher et al., 2014) or have concentrated on a single site (Chen et al., 2021a, 2019; Zhang et al., 2020b, 2019), the seasonal pattern and regional variability of this response remain largely unknown, especially when the cold seasons have a faster warming rate (Yang et al., 2010).

Qinghai-Tibetan Plateau (QTP) soils have large carbon stocks, with >48 Pg carbon estimated in the top 1 m of soil (Chen et al., 2022). Nevertheless, whether the QTP operates as a CH_4 sink or source and its magnitude still have no consistent conclusion. Being the primary contributions of CH_4 sources and sinks in the QTP, the wetlands (including vegetated wetlands, marshes, and peatlands) are a net source of 0.16–2.37 Tg C yr⁻¹ (Fig. S1, Table S1), and the grasslands (including steppes and meadows) are a weak source or sink of –0.55–0.10 Tg C yr⁻¹ (Fig. S1, Table S2), as documented by historical measurements and simulations. With a warming rate of ~0.4 °C per decade (around twice the global mean), the QTP has experienced unprecedented environmental changes and permafrost degradations since the 1970s (Bibi et al., 2018; Chen et al., 2022). This has led to both shrinkage and expansion of wetlands and grasslands on the QTP (Chen et al., 2013; Wang et al., 2020b; Wei and Wang, 2017; Zhao and Zhang, 2015), increasing the uncertainty of the CH_4 budget on the QTP.

Numerous studies have demonstrated that the amplitude of CH_4 fluxes is primarily driven by temperature, with CH_4 flux increasing as temperatures rise (Song et al., 2009; Wille et al., 2008). Because of the cold and dry winter (Wu and Zhang, 2008), the non-growing season of QTP is vulnerable to warming, which is twice as much as the annual average warming (Yang et al., 2010). The CH_4 emissions and uptakes of the QTP will respond to climate warming, especially during the non-growing season. However, the measurements of QTP mainly focused on the growing season, and there is a lack of continuous observations on the non-growing seasons (Wang et al., 2014; Zhang et al., 2019). Research based on global measurements shows that the sensitivity of

CH_4 emission from wetlands is correlated with soil temperatures, and reach the maximum in summer (Li et al., 2023a). It is unknown yet whether this response to global warming is consistent between the growing season and non-growing seasons of the QTP, and whether it is consistent between the QTP and world average (Li et al., 2023a).

Warming experiments are effective approaches for studying the temperature sensitivity of CH_4 exchange, yet they are less common across QTP sites (Chen et al., 2017; Wang et al., 2022, 2021). Most sites solely conduct continuous observation of CH_4 exchange, soil temperature, and other environment factors (Peng et al., 2019; Wu et al., 2021; Yao et al., 2019). CH_4 exchange in response to soil temperature can be regressed by liner or exponential function models (Bao et al., 2021; Yao et al., 2019). However, significant uncertainties may arise from the neglect of environmental differences among sites (Richardson et al., 2006). Mixed-effects models stand out for meta-analyses due to their ability to handle nested covariance structures and accommodate unbalanced designs (Yvon-Durocher et al., 2014). These models facilitate comprehensive data integration across sites. In addition, mechanistic and machine learning models can be used to simulate real experiments and scale CH_4 fluxes from sites to region. Mechanistic models have been used to simulate CH_4 fluxes as the sum of CH_4 generation and oxidation processes, yet uncertainties persist due to unclear mechanisms (Ito and Inatomi, 2012; Li et al., 2020b). Conversely, machine learning models understand intricate relationships among CH_4 flux, soil temperature, and other factors, effectively simulating CH_4 flux based on observed data (Kim et al., 2020).

Here, we examined the seasonal temperature dependencies of CH_4 in wetlands and grasslands across the QTP, aiming to answer the following questions: (i) What is the general seasonal pattern of temperature dependencies of CH_4 fluxes from wetlands and grasslands on the QTP? (ii) How does the seasonality affect CH_4 source/sink in wetlands and grasslands on the QTP with soil warming? We obtained 9745 daily observations of CH_4 fluxes from 27 sites across the QTP, encompassing both wetlands and grasslands. The seasonality of CH_4 exchange warming responses in QTP wetlands and grasslands was analyzed based on four methods: regression fitting of temperature- CH_4 flux, temperature dependence calculations, field-based and model-based control experiments.

2. Materials and methods

2.1. Data collection

We collected 9745 daily observations of CH_4 fluxes from 27 sites (Fig. 1; Table S3) across wetlands and grasslands on the QTP (Liu et al., 2023). The CH_4 fluxes were derived from two distinct sources (raw data and literature-based data) based on three measurement methodologies.

The raw data was obtained by directly contacting the researchers or accessing public data sets. Literature-based data were collated through targeted searches on Web of Science (<https://www.webofscience.com/>) and the China National Knowledge Infrastructure (<https://www.cnki.net/>) using specific keywords such as methane, soil temperature, and Tibetan Plateau. Three measurement methodologies contain the traditional discrete Manual Static Chamber (MSC) (17 sites, Table S4), Continuous Automated Chamber (CAC) (2 sites, Table S5) and Eddy Covariance (EC) (8 sites, Table S6).

For the CAC data, fluxes with level 2 and 3 flags, fluxes with $p > 0.05$ for the regression of CO_2 , and fluxes beyond the range of 99 % of the filtered data were excluded (Wang et al., 2022) (Table S5). For the eddy covariance (EC) data, the data processing software (EddyPro, LI-COR Inc.) was used for coordinate axis rotation and Webb-Pearman-Leuning (WPL) correction (Table S6). Data affected by rain and instrument malfunction, or collected during periods of weak turbulence were removed. Additionally, fluxes covering <8 h in a day were excluded before computing the daily CH_4 fluxes.

Literature-based data were obtained from the text, tables, figures, and appendices of the papers. Extraction from figures was facilitated using GetData Graph Digitizer (version 2.25, <http://www.getdata-graph-digitizer.com>). For each paper, we recorded the daily CH_4 flux and soil temperature data. The R^2 between the extracted data and the raw data based on the three measurement approaches is over 0.9 (Fig. S2). These peer-reviewed data have been applied to a series of postprocessed and quality-controlled procedures prior to publication. The extracted observations are treated as extreme outliers and have been removed if they exceed three times the interquartile range below the first quartile (Q1) or above the third quartile (Q3) (Krzewinski and Altman, 2014). Table S3 contains the amount of valid data for each variable.

The sites cover most of the wetland and grassland ecosystem types in the QTP, which include alpine marsh (2 sites), alpine wetland (8 sites), fen (2 sites), swamp meadow (1 site), alpine steppe (5 sites), and alpine meadow (9 sites). Most sites were in the central and eastern QTP (Fig. 1). Due to the bad climate and very limited road traffic, there are few observation data in the west and north of QTP. 13 sites are between 3000 and 3500 m above sea level (asl), four sites are between 3500 and 4000 m asl, and eight sites are between 4000 and 5000 m asl (two sites have no altitude information). These include 19 discontinuous and 8 sporadic permafrost sites (Brown et al., 2002). The sampling frequencies of CH_4 flux varied among sites due to different observation methods. The sampling frequencies of the EC and CAC system are once per 30 min or every per hour (Tables S5 and S6). The sampling frequencies of the MSC technique is once per day, once per week, or once per month (Table S4).

2.2. Integration analysis

Of the 27 sites collected, seven sites lacked soil temperature mea-

surements (Table S3), which were only used to study seasonal variation of CH_4 exchange. For the other 20 sites with soil temperature data, we used linear and exponential regression to explore the relationship between soil temperature and CH_4 exchange. Only sites displaying significant regression ($p < 0.05$) were considered for temperature dependence calculations and machine learning modeling. The sensitive coefficient of CH_4 fluxes in response to soil temperature was determined by the *Slope* and the Q_{10} value. The *Slope* is slope coefficient in linear regression function. The Q_{10} value is calculated with exponential efflux-temperature relationship $Q_{10} = e^{10b}$, where b is the regression coefficient fitted. Relationships were fitted from means between sites calculated over equally spaced ($1\text{ }^\circ\text{C}$) bins (Wang et al., 2020a).

There are significant disparities in the response of CH_4 fluxes to soil temperature across the studies sites (Fig. S3). To address this issue, we set up two types of mixed-effect model analyses: first, the fixed effects representing the average temperature response of CH_4 exchanges across all sites (Fig. 4a and c); and second, the random effects representing the magnitudes of the deviations from these fixed effects for each of the sites (Fig. 4b and d). The linear mixed-effects modeling was employed based on a Boltzmann-Arrhenius function, as described by Yvon-Durocher et al. (2014):

$$\ln R_i(T) = (\bar{E} + \epsilon_E^i) \left(\frac{1}{kT_C} - \frac{1}{kT} \right) + (\ln R(T_C) + \epsilon_R^i) \quad (1)$$

where $\ln R_i(T)$ represents the natural logarithm of the CH_4 flux at absolute temperature T (K) for arbitrary site i . \bar{E} , is the average apparent activation energy (eV) among sites, which represents the temperature dependence of CH_4 fluxes. k is the Boltzmann constant (8.62×10^{-5} eV K^{-1}). $\ln R(T_C)$ represents the average of natural logarithm of CH_4 flux across all sites at mean soil temperature T_C .

Biotic factors (substrate supply, microbial community structure and/or composition, physiological acclimation and/or adaptation) and abiotic factors (mean annual air temperature, soil moisture) may regulate CH_4 emission and uptake in response to ambient temperature differently at different sites. Thus, the apparent activation energy (E) and the natural logarithm of CH_4 fluxes at a fixed temperature ($\ln R(T_c)$) are expected to vary. The linear mixed-effects models accounted for variations by treating slopes and intercepts as random variables with averages of \bar{E} and $\ln R(T_C)$, respectively. Site-specific deviations were defined as ϵ_E^i and ϵ_R^i for each site, i . The linear mixed-effects modeling analysis was performed using the ‘curve_fit’ function inside the ‘scipy’ package in Python. Sites with less than five data points were removed from the analysis. In addition, we standardized the data by subtracting the estimated rate at the average temperature of the total data.

2.3. Field- and model-based control experiments

The integration of controlled experiments involved three sites

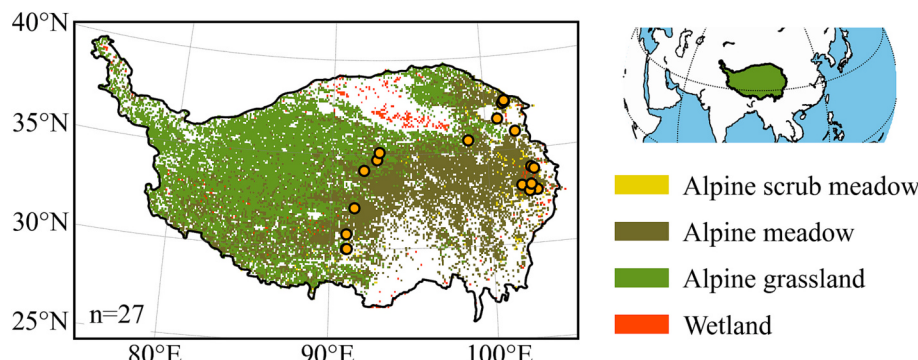


Fig. 1. Locations and vegetation types of the 27 sites on the QTP. The map at the top right shows the location of the QTP (colored in green). The vegetation map was developed by Zhou et al. (2023). The alpine scrub meadow, alpine meadow, and alpine grassland are classified as grassland in this study.

(Hongyuan #1, Hongyuan #2, and Fenghuoshan, as listed in Table S3) where manipulative warming experiments were conducted (Chen et al., 2017; Wang et al., 2021, 2022). The response of CH₄ flux to warming was indicated by RR_{CH_4} , where $RR_{CH_4} = \left(\frac{R_{CH_4\text{warming}} - R_{CH_4\text{control}}}{R_{CH_4\text{warming}}} \right) / R_{CH_4\text{warming}} \times S$. S is a binary value, with 1 and -1 representing the CH₄ source and sink under warming treatments, respectively.

We developed a data-driven machine learning (ML) model to assess the effects of soil temperature on CH₄ fluxes across the QTP. The ensemble regression tree random forest (RF) model measures “variable importance” by permuting a predictor variable (Breiman, 2001). In CH₄ flux upscaling (Bodesheim et al., 2018) and gap-filling (Kim et al., 2020; Wang et al., 2022) studies, the RF model outperforms other ML algorithms. We designed five simulation cases with an increase of daily soil temperature by +0 °C (control), +0.5 °C, +1.0 °C, +1.5 °C, and +2.0 °C, respectively.

The driving variables of the RF model include net ecosystem productivity (NEP), water table height (WTH), soil water content (SWC), soil temperature (Ts), friction velocity (U), and latent heat flux (LE) (Table S7), following Kim et al. (2020). After normalization, regression trees were built using the “sklearn” Python extension package. The RF model was trained using the collected observations and then scaled up to the entire QTP based on regional data (Table S7). The measurements were randomly separated into a training set (80 %) and a test set (20 %) to train and test the model. The CH₄ fluxes of wetlands and grasslands were simulated respectively. Vegetation types of these sites and regions were collected from the publications (Table S3) and the vegetation maps (Zhou et al., 2023).

2.4. Division of seasons

According to the description of the original documents of each site, the whole year was divided into growing season and non-growing season (Fig. S2, and Table S3). The purpose of this division is to test the seasonality of CH₄ exchanges temperature response. The seasonal division for CH₄-related studies on the QTP is mainly based on (i) soil temperature change (the whole year is split into frozen, thawing, thawed, and freezing seasons), (ii) Julian day, (iii) vegetation phenology change, and (iv) microbial activity, etc. (Fig. S4). For one site (Naqu) where seasonal divisions were not specified in the papers, we employed MODIS MCD12Q2 phenology data (Running et al., 2021) for the division. The seasonal division based on remote sensing is roughly compatible with the seasonal division based on literature (Fig. S5).

3. Results

3.1. Seasonal variations of CH₄ fluxes with soil temperature

Based on the sites with both CH₄ fluxes and soil temperature measurements (Table S3), wetland CH₄ fluxes rose exponentially ($p < 0.001$) with soil temperature (Fig. 2a) and reached the peak during the growing season (Fig. 3a). The estimated Q_{10} value is higher during non-growing season ($Q_{10} = 4.10 \pm 1.00$) than the growing season ($Q_{10} = 2.20 \pm 1.00$), indicating higher soil temperature sensitivity of the non-growing growing season CH₄ emission (Fig. 2a). The CH₄ flux in the growing season ($\bar{R}_{CH_4} = 151.17 \pm 227.81 \text{ mg C m}^{-2} \text{ d}^{-1}$) was significantly ($p < 0.001$) higher than that in the non-growing season ($\bar{R}_{CH_4} = 34.46 \pm 28.74 \text{ mg C m}^{-2} \text{ d}^{-1}$) (Fig. 3b).

The CH₄ source/sink state varied during different periods of one year in the grassland sites on the QTP (Fig. 3c). The growing season was shown as a CH₄ sink ($\bar{R}_{CH_4} = -2.44 \pm 5.58 \text{ mg C m}^{-2} \text{ d}^{-1}$), while the non-growing is shown as a CH₄ source ($\bar{R}_{CH_4} = 1.61 \pm 6.11 \text{ mg C m}^{-2} \text{ d}^{-1}$) (Fig. 3d). The primary CH₄ emissions were observed during late growing seasons, as well as in the non-growing seasons of winter and spring. Conversely, predominant CH₄ uptake was observed in the early

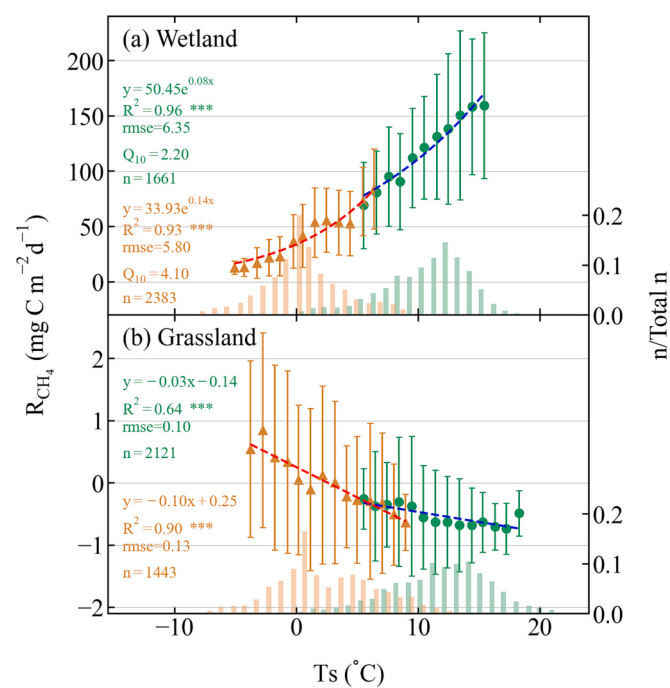


Fig. 2. Variations of daily CH₄ fluxes (R_{CH_4}) with daily mean soil temperature (Ts) across the wetland (a) and grassland sites (b) on the QTP for growing seasons (GS) and non-growing seasons (NGS). Mean values of R_{CH_4} were calculated at binned Ts values of 1 °C intervals for GS (green circle) and NGS (brown triangle). Vertical lines represent \pm std. and vertical bars represent the frequency distributions with a total n of 1661 (GS of wetland), 2382 (NGS of wetland), 2121 (GS of grassland), and 1443 (NGS of grassland). Data were excluded when the n was less than half of mean n for all binned intervals. The dash lines are the fitted curves of GS (blue) and NGS (red) based on the means of equally spaced bins. Texts represent information about the fitted lines. *** indicates the significance ($p < 0.001$) of the fitted curves. Sites without significant linear or exponential relationship between CH₄ flux and soil temperature during the growing season and non-growing season have been removed (Fig. S6, S7, and S8).

growing seasons and during non-growing periods in autumn and winter. There was a significant negative correlation between soil temperature and CH₄ flux in grassland sites (Fig. 2b). The fitted Slope value of non-growing season (-0.10 ± 0.01) is smaller than that of growing season (-0.03 ± 0.007). With rising soil temperatures, the transition from CH₄ source to sink during the non-growing season occurs at a faster rate than the increase of CH₄ uptake during the growing season. Two grassland sites without significant linear or exponential relationships between CH₄ flux and soil temperature during the growing season and non-growing season have been removed (Fig. S6, S7 and S8).

We employed the Boltzmann-Arrhenius function to further assess the relationship between soil temperature and CH₄ flux (Fig. 4). At wetland sites, the non-growing season has a higher apparent activation energy ($\bar{E} = 1.01 \pm 0.05$) than the growing season ($\bar{E} = 0.57 \pm 0.03$) for CH₄ emission, indicating a larger temperature dependency (Fig. 4a). The mean activation energy in the growing season (1.17 ± 0.70 eV) is significantly greater than that in the non-growing season (-0.12 ± 1.54 eV) (Fig. 4b). At grassland sites, the non-growing season has a higher apparent activation energy ($\bar{E} = 0.44 \pm 0.04$) than the growing season ($\bar{E} = 0.08 \pm 0.03$) for CH₄ uptake, indicating a larger temperature dependency (Fig. 4c). The mean activation energy in the growing season (0.51 ± 0.22 eV) is significantly greater than that in the non-growing season (0.15 ± 0.33 eV) (Fig. 4d). Due to the fewer site-years, mixed-effect analysis cannot effectively analyze the activation energy of CH₄ uptake in wetlands and CH₄ release in grasslands on soil temperature (Fig. S9).

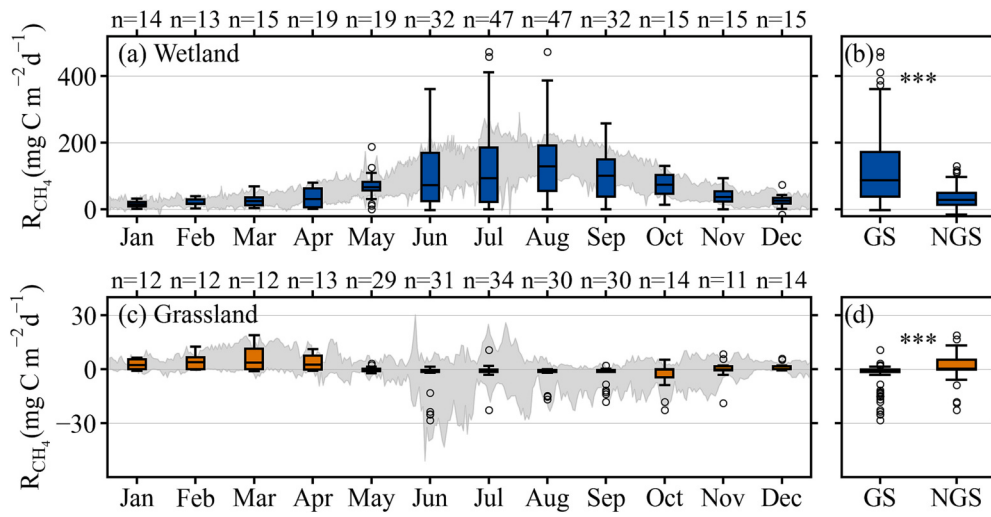


Fig. 3. Seasonal variations and magnitudes of the CH_4 fluxes (R_{CH_4}) across the QTP wetland sites (a and b) and grassland sites (c and d). The boxplots in (a) and (c) represent the monthly mean CH_4 fluxes across the QTP wetland sites and grassland sites, respectively. The n on the top axis represents the number of monthly means. The gray shading represents the daily R_{CH_4} across the QTP wetland sites (a) and grassland sites (c), respectively. The boxplots in (b) and (d) represent total CH_4 fluxes during growing (GS) and non-growing (NGS) seasons for the wetland sites (b) and grassland sites (d), respectively. *** means that there is a significant difference ($p < 0.001$) in the t -test CH_4 flux between growing season and non-growing season.

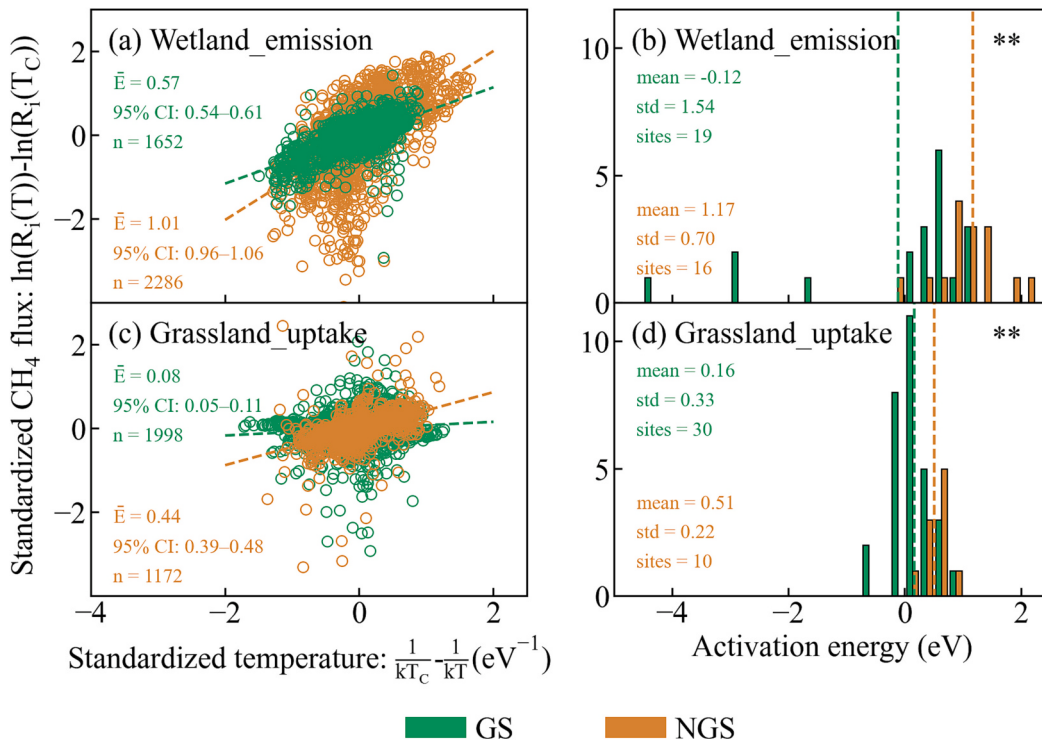


Fig. 4. Temperature dependence of the CH_4 flux (R_{CH_4}). Temperature dependencies are characterized in (a and c) by fitting a Boltzmann-Arrhenius function with site ensemble random effects. The fitted dashed line in (a and c) corresponds to the \bar{E} . All the fitted lines are significant ($p < 0.05$). The distribution of site-level temperature dependence is presented as a histogram of slope estimates in (b and d). The dashed line in (b and d) represents the mean apparent activation energy among sites. Data in (a and c) have been standardized by subtracting the estimated site-specific intercept from each measurement; that is, the estimated CH_4 flux at a fixed temperature, $\ln R(T_c)$, where T_c is the average temperature for the site-level data. ** means that there is a significant difference ($p < 0.01$) in the t -test CH_4 flux between growing season and non-growing season.

3.2. Warming impacts on CH_4 exchange

The response of CH_4 fluxes to experimental warming was investigated by analyzing three controlled warming experiments conducted at the grassland sites (Chen et al., 2017; Wang et al., 2021, 2022). 91.42 % and 97.41 % of daily CH_4 uptake was intensified by experimental

warming compared to the control condition in the growing and non-growing season, respectively (Fig. 5). Warming led to a significant rise of daily CH_4 uptake, with a mean RR_{CH_4} of -0.19 ± 0.16 during the growing season and -0.44 ± 0.26 during the non-growing season (Fig. 5c). The soil temperature rose more significantly during the non-growing season (4.75 ± 2.50 °C) than the growing season

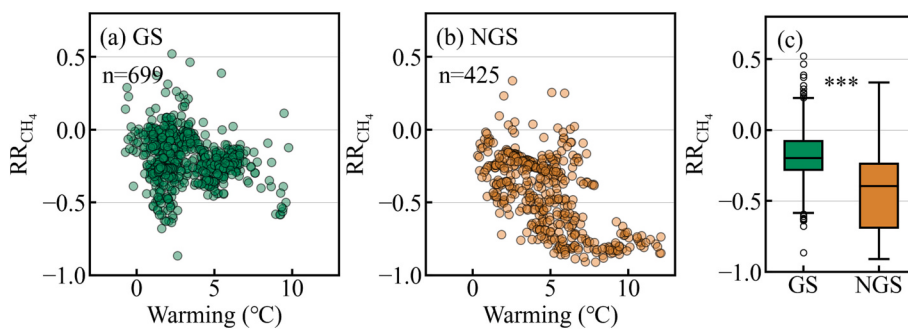


Fig. 5. Response of CH_4 flux (RR_{CH_4}) to experimental warming across 3 manipulative warming experiments at the grassland sites on the QTP for the growing season (a) and non-growing season (b). $\text{RR}_{\text{CH}_4} > 0$ and $\text{RR}_{\text{CH}_4} < 0$ indicate the CH_4 emission and uptake have been promoted by soil warming, respectively. (c) is the mean response of CH_4 flux to experimental warming from (a) and (b). Each point in the figure represents daily data for each experiment. *** means that there is a significant difference ($p < 0.001$) in the t -test CH_4 flux between growing season and non-growing season.

(3.22 ± 2.01 °C) under identical warming treatments.

Simulated warming increased CH_4 flux mostly occurred during the non-growing season, especially for the transitional periods between seasons (Fig. 6). The simulated CH_4 emission increased with soil temperature for wetlands. The simulated CH_4 uptake also increased with soil temperature for grasslands. The ML model demonstrated that the variability of daily CH_4 exchange in wetlands can be effectively explained by the variable Ts, with an importance value of 0.53 (Fig. 7a). Conversely, in grasslands, the most influential variables are WTD, Ts, and LE, with important values of 0.38, 0.17, and 0.15, respectively (Fig. 7b). The correlation coefficient (R^2) between observed and simulated CH_4 concentrations is 0.81 for wetlands (Fig. S10a) and 0.64 for grasslands (Fig. S10b).

In wetlands, there is no significant difference between the +0.5 °C and +1.0 °C warming cases and the control (+0 °C) for CH_4 exchange both for the growth and non-growing seasons ($p > 0.05$). However, there is a significant ($p < 0.05$) increase in CH_4 exchange under the +1.5 °C and +2.0 °C warming cases (Fig. 6a). In +0.5 °C, +1.0 °C, +1.5 °C, and +2.0 °C warming cases, the yearly average ΔR_{CH_4} was 1.30 ± 1.11 , 2.70 ± 2.29 , 4.07 ± 3.43 , and 5.35 ± 4.51 mg C m⁻², respectively. The

average ΔR_{CH_4} of the non-growing season was greater than that of the growing season, and the difference between the two rose progressively with controlled warming, with an average of 2.77 times and a maximum of 3.26 times in the +2.0 °C warming case.

In grasslands, there is no significant difference between the +0.5 °C, +1.0 °C, and +1.5 °C warming cases and the control (+0 °C) for CH_4 exchange during the growing season ($p > 0.05$). However, during the non-growing season, there is a significant difference ($p < 0.05$) in CH_4 exchange between the +1.0 °C, +1.5 °C, and +2.0 °C warming cases and the control. In +0.5 °C, +1.0 °C, +1.5 °C, and +2.0 °C warming cases, the yearly average ΔR_{CH_4} was -0.07 ± 0.09 , -0.14 ± 0.18 , -0.21 ± 0.27 , and -0.28 ± 0.35 mg C m⁻², respectively. The absolute value of average ΔR_{CH_4} of the non-growing season was greater than that of the growing season, and the difference between the two rose progressively with controlled warming, with an average of 5.53 times and a maximum of 6.34 times in the +2.0 °C warming case.

In the non-growing season, especially in the shoulder season, the change of CH_4 exchange caused by climate warming accounts for a large proportion of the annual changes (Fig. 6). In wetlands, the mean proportion of ΔR_{CH_4} in the non-growing season to the total annual variation is 79.11 %, whereas in grasslands, the mean proportion is 88.34 %.

4. Discussion

4.1. Nonnegligible enhanced CH_4 exchanges in the non-growing season

We integrated 9745 daily CH_4 fluxes observations and found a more pronounced warming response in CH_4 source/sink dynamics on the QTP during the non-growing season compared to the typical growing season. Warming elevated CH_4 emissions from wetlands, showing an average reaction intensity in the non-growing season 1.89 times higher than in the growing season (average value of $Q_{10 \text{ NGS}}/Q_{10 \text{ GS}}$, $\bar{E}_{\text{NGS}}/\bar{E}_{\text{GS}}$, and $\Delta \bar{R}_{\text{NGS}}/\Delta \bar{R}_{\text{GS}}$). Lower CH_4 emissions in the non-growing season were mainly due to inhibited activity of methanogenic bacteria and formation of CH_4 owing to lower temperatures (Wei et al., 2015). Rising temperature spurred dormant microorganisms, leading to additional CH_4 emissions from soil (Chadburn et al., 2020; Chen et al., 2021b). Increased water resources from early thawing and delayed freezing of QTP wetlands may limit the oxygen concentration, creating more anaerobic conditions, boosting CH_4 production and emission while inhibiting CH_4 aerobic oxidation (Zhang et al., 2020a, 2020b). The rise in emission corresponds to a “burst” in the early thawing season, releasing accumulated CH_4 after winter soil thawing (Arndt et al., 2020). Notably, significant CH_4 emission bursts were observed near 0 °C at some wetlands sites (Fig. S8). Climate-induced prolongation of thawing seasons may advance this “burst”, consequently increasing CH_4 emissions in non-growing season.

Warming promoted CH_4 uptakes from grasslands, and the average

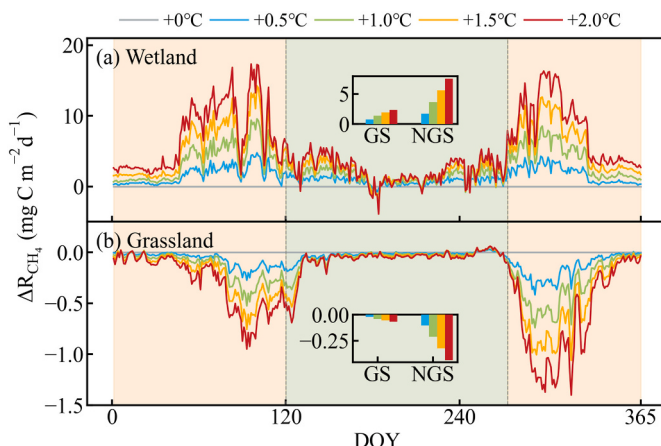


Fig. 6. Warming-induced variation in daily delta CH_4 fluxes (ΔR_{CH_4}) between cases of wetland (a) and grassland (b) on the QTP. The bar chart subplot represents the average ΔR_{CH_4} for growing (GS) and non-growing (NGS) seasons, respectively. Lines and bars with different colors indicate the difference between control case and different warming case. The data is stimulated by the RF model through five warming cases (+0 °C, +0.5 °C, +1.0 °C, +1.5 °C, +2.0 °C). The shaded background in green between DOY 121–273 represents the growing season, and the shaded background in light orange between DOY 1–120 and DOY 274–365 represents the non-growing season. This seasonal division is used for visualization and comparisons only. This division scheme is the most used one in the sites (11/27 sites, reference in Fig. S3 and Table S3).

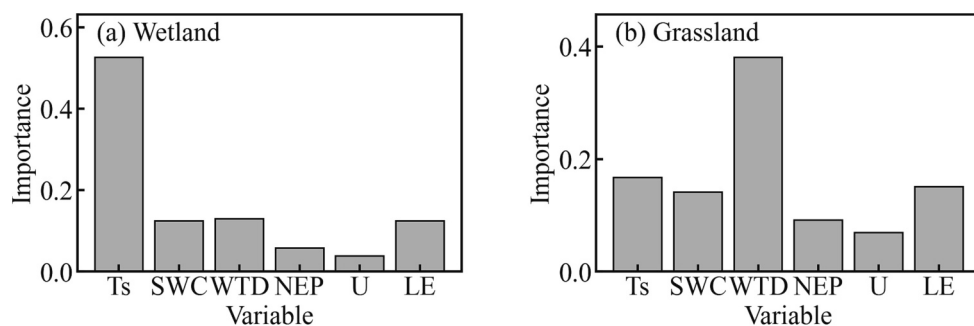


Fig. 7. Variable importance for the machine learning (ML) model in wetland (a) and grassland (b) sites in the QTP. The variables contain soil temperature (Ts), soil water content (SWC), water table depth (WTD), net ecosystem productivity (NEP), friction velocity (U), and latent heat flux (LE) (Table S7).

reaction intensity in the non-growing season is 4.80 times greater than that in the growing season (average value of $Slope_{NGS}/Slope_{GS}$, $\bar{R}_{NGS}/\bar{R}_{GS}$, $\bar{E}_{NGS}/\bar{E}_{GS}$, and $\Delta\bar{R}_{NGS}/\Delta\bar{R}_{GS}$). The CH₄ uptake in grasslands on the QTP could be attributed to methanotroph oxidation, influenced by methanotroph activity and substrate availability (King, 1997; Le Mer and Roger, 2001; Segers, 1998). The methanotroph community is affected by temperature and soil aerobic conditions (Conrad, 2007), with CH₄ consumption rising temperature (Zhuang et al., 2013). Frozen soil could constrain CH₄ and O₂ diffusion, reducing methanotrophic substrates and CH₄ uptake. Warming extends soil thawing, releasing methanotrophs from substrate limitation, fostering a strong CH₄ sink in oxygenated warmed soil. The positive effect of warming on CH₄ uptake till the rainy season may stem from soil drying, which may lead to the acceleration of CH₄ and O₂ diffusion (Wei et al., 2015). Subsequent rainfall weakens the effect of warming on CH₄ uptake. Variation in groundwater depth and soil moisture, therefore, heavily impact CH₄ and O₂ exchange and the methanotroph community (Curry, 2007; Zhuang et al., 2013). Warming increases evapotranspiration, creating a drier, aerated soil with greater diffusivity and more substrates (CH₄ and O₂), potentially boosting methanotroph abundance and altering their structure (Li et al., 2020a; Zhang et al., 2021; Zheng et al., 2012).

The monthly temperature dependence of CH₄ fluxes in the growing season is also lower than that in the non-growing season on the QTP (Fig. S11). Li et al. (2023a) have found warm months have a higher temperature dependence of CH₄ emissions compared to cold months. This study was based on 42 widely distributed wetlands globally from the FLUXNET-CH₄ database, but it lacks measurements in the QTP. Globally, increased temperatures may lead to greater vegetation productivity, which indirectly contributes to increased CH₄ emissions in the growing season by affecting substrate availability (Li et al., 2023a). However, compared to other tropical and boreal cold regions, the climate of the QTP is unique. There is no continuous snowpack in the non-growing season, and precipitation is mainly in the growing season (Wu and Zhang, 2008). That leads to dry winters and humid summers. In addition, the degradation of permafrost could lead to the decrease of soil moisture, and even reduce the contribution of summer warming to vegetation productivity (Jin et al., 2021). Soil warming and its accompanying effects have a greater impact on CH₄ emissions than the effect of vegetation productivity on the QTP, and thus CH₄ exchange has the strongest response to warming in the non-growing season (Li et al., 2022).

4.2. Increased uncertainty of CH₄ budget on the QTP

The QTP is experiencing unprecedented climate change, with a more rapid warming rate (0.4 °C per decade) than the global average and high-latitude permafrost (Biskaborn et al., 2019; Li et al., 2023b; Ran et al., 2018) and a twice of winter warming rate than the annual average (Yang et al., 2010). However, the CH₄ exchange response to warming on the QTP may have been underestimated with very limited

measurements in non-growing seasons because of poor accessibility to some stations (Wei et al., 2015). A fixed contribution factor of ~30 % was applied to some grassland sites for the non-growing season (Wei et al., 2015; Zhang et al., 2019). The annual CH₄ budget had not even taken into account the CH₄ emissions during the non-growing season at some stations (Wang et al., 2014). However, in the context of climate warming on the QTP, this proportion may be changed and the CH₄ flux in the non-growing season will be non-negligible (Peng et al., 2019).

Previous research on the temperature dependence of ecosystem-level CH₄ emissions has shown a wide range of apparent activation energies, spanning from 0.2 to 2.5 eV (1 eV = 96 kJ mol⁻¹) (Chen et al., 2021b). Yvon-Durocher et al. (2014) showed that the average temperature dependence of CH₄ for the global 127 field wetland sites is 0.96 eV. This value is higher than the average activation energy we calculated for the whole year of wetlands (0.84 eV) (Fig. S12a), but lower than the average activation energy of the non-growing season ($\bar{E} = 1.01$) (Fig. 4a). In addition, the activation energy of CH₄ calculated for grasslands in our study is also much lower than that for wetlands (Fig. 4 and S12). Groundwater depth and soil moisture may be important factors affecting CH₄ exchange in grasslands due to relatively dry environment. The increase of soil moisture caused by permafrost degradation and the decrease of soil moisture caused by seasonal frozen soil degradation may increase the uncertainty of grassland CH₄ response to soil temperature.

The magnitude of CH₄ flux and its response to warming is spatially distributed due to the biotic and abiotic factors, such as NEP, WTH, SWC, Ts, U, and LE (Fig. S13) (Qin et al., 2014). The fraction of non-growing season cumulative CH₄ emission to the total annual emission varied from 6 % to 47 % in different sites of the QTP (Peng et al., 2019; Song et al., 2015; Treat et al., 2018; Wu et al., 2021). The midwestern QTP has larger annual amplitudes (Fig. S14) and stronger warming responses (Fig. S15) of simulated CH₄ fluxes with regionally homogeneous warming. The midwestern QTP has been predicted to become significantly warmer than the eastern QTP (Li et al., 2023b), and that will further increase the spatial difference of CH₄ source/sink on the QTP.

With climate warming, wetlands and grasslands on the QTP have been experiencing continued expansion (Wang et al., 2020b; Wei and Wang, 2017; Zhao and Zhang, 2015) and shrinking (Chen et al., 2013; Wang et al., 2020b; Zhao and Zhang, 2015), and this will result in increasing uncertainty of CH₄ emissions and uptakes on the QTP. Extensive and rapid retreat and thinning of permafrost could accelerate biogeochemical processes, turning these cold wetlands into net sources of CH₄ (Yang et al., 2010). The progressive increase in active layer thickness could also cause ecosystem desertification in the QTP, reducing CH₄ production and release with degraded alpine wetland and grassland, which already appeared in the eastern and western portions of QTP (Yang et al., 2010).

Additionally, the cold and dry winter without a continuous snowpack of the QTP could lead to more sensitive F-T cycles to increasing temperatures in the winter (Chen et al., 2020; Wu and Zhang, 2008). Uncertainty in the CH₄ budget of the QTP under a warming scenario will

therefore increase dramatically, especially during the non-growing season. Under the +5 °C case, the wetland and grassland on the QTP changed by 5.35 mg C m⁻² d⁻¹ and -0.28 mg C m⁻² d⁻¹, respectively, with the non-growing season contributing 79.11 % and 88.34 %, respectively (Fig. S14).

4.3. Uncertainty and outlook

The CH₄ exchange for the 27 sites were measured using the manual static chamber, continuous automated chamber, and eddy covariance methods respectively (Table S3). The accuracy of the three monitoring techniques is not consistent with each other (Long et al., 2010). We analyzed the relative differences between growing season and non-growing seasons to avoid the difference in the value and accuracy of CH₄ flux. The mixed-effect model is also used to reduce this effect. However, effects such as chamber effects (Yu et al., 2013) and low turbulence (Long et al., 2010) may even change the actual relationship between soil temperature and CH₄ exchange. We collected observations from only 27 sites, 17 of which used the traditional discrete Manual Static Chamber (Table S3). The installation of this chamber may change temperature and pressure, thus altering the gas diffusion gradient within the soil profile (Koskinen et al., 2014). Usually, measurements with the MSC technique can only be operated during the growing season due to the poor environment on the QTP. And its observations are not continuous in time. These limitations will bring significant impacts on the analysis of CH₄ exchange and its temperature sensitivity. Thus, continuous measurements using the CAC and EC technique with a direct signal of land-atmosphere CH₄ exchange are ideally suited for time series analysis (Baldocchi et al., 2001; Peng et al., 2019). Although CAC method remains the chamber effect, it is suitable for analyzing the effect of soil warming on CH₄ flux because it reduced the influence of air flow (Wang et al., 2021). Measurements based on EC technology can be affected by radiation and turbulence, but incorporating environmental influences is suitable for multi-factor analysis (Yu et al., 2013). Characteristics of different technologies should be reasonably considered in future CH₄ measurement.

Methane exchange is affected by various environmental factors, including soil temperature, moisture, and substrate supply (Qin et al., 2014). In this study, we compared four methods to analyze its response to temperature changes. The bin average method groups data into uniform bins, helping minimize the impacts of other environmental factors (Wang et al., 2020a). Mixed-effects models treat slopes and intercepts as random variables, accounting for site-specific variations. Site-unit-level relationships are nested within overall relationships (Yvon-Durocher et al., 2014). We employed two types of mixed-effect model analyses—site-ensemble and site-specific—to minimize differences between sites. The field-based and model-based controlled studies isolated temperature changes, maintaining other factors constant, enabling specific analysis of methane exchange responses to temperature alterations (Wang et al., 2022). While these methods reduce the impact of environmental factors, one should keep in mind that the response of methane exchange to temperature is still accompanied by changes in other relevant factors (Li et al., 2023a).

Traditional CH₄ modules in biogeochemistry models focus less on CH₄ uptake, which makes an important contribution to the CH₄ budget on the QTP, and more on CH₄ emissions (Bohn et al., 2015; Li et al., 2020b; Salmon et al., 2022; Watts et al., 2023). One key reason is the high uncertainty of models in the mechanism of CH₄ oxidation and associated processes due to a lack of detailed validation with regional CH₄ uptake observations (Watts et al., 2023; Yu et al., 2017). Warming will significantly increase QTP grassland CH₄ uptake, and thus the CH₄ oxidative module in the biogeochemical model should be given increasing consideration. Numerical simulations indicated that air temperature on the QTP will continue to increase in the 21st century (Yang et al., 2010), and the occurrence of extreme climate and thermal karst will probably increase, which will introduce more uncertainties in

the predictions of CH₄ exchange. Therefore, a clear understanding of the seasonality of CH₄ exchange and its response to soil warming will be beneficial to the estimation of the CH₄ budget over the QTP.

5. Conclusions

In conclusion, our study emphasized a heightened warming response in CH₄ exchange during the non-growing season in the wetlands and grasslands on the QTP. Wetlands exhibited a 1.89 times stronger average CH₄ emission reaction intensity in the non-growing season compared to the growing season, while grasslands showed a 4.80 times greater intensity in CH₄ uptake during the non-growing season. This stronger warming effect led to increased CH₄ source/sink dynamics during the non-growing season. The temperature-driven CH₄ exchange on the QTP displayed different seasonal patterns than global wetlands, which exhibiting stronger dependencies during the warmer growing season (Li et al., 2023a). As global warming prolongs thawing seasons, it is expected to amplify this effect, heightening annual CH₄ exchange. Neglecting the seasonality of warming response of CH₄ exchange could introduce significant modeling errors in assessing the CH₄ source/sink dynamics over the QTP under climate warming. The QTP experiences rapid and asymmetric warming, escalating at 0.4 °C per decade over 50 years, with winter warming doubling the annual average. Such unprecedented warming necessitates a more meticulous consideration of CH₄ exchange responses in model simulations.

CRediT authorship contribution statement

Zhenhai Liu: Writing – original draft, Visualization, Validation, Software, Methodology, Formal analysis, Data curation, Conceptualization. **Bin Chen:** Writing – review & editing, Supervision, Project administration. **Shaoqiang Wang:** Writing – review & editing, Supervision, Project administration. **Xiyan Xu:** Writing – review & editing. **Huai Chen:** Data curation. **Xinwei Liu:** Data curation. **Jin-Sheng He:** Data curation. **Jinsong Wang:** Data curation. **Jinghua Chen:** Writing – review & editing. **Chen Zheng:** Data curation. **Kai Zhu:** Data curation. **Xueqing Wang:** Data curation.

Declaration of competing interest

The authors declare the following financial interests/personal relationships which may be considered as potential competing interests:

Shaoqiang Wang reports financial support was provided by the Provincial Government of Qinghai, China. Bin Chen reports financial support was provided by the Key Laboratory of Coupling Process and Effect of Natural Resources Elements. Bin Chen reports equipment, drugs, or supplies was provided by the National Key Scientific and Technological Infrastructure project.

Data availability

The collected observations of CH₄ fluxes from 27 sites on the QTP are available at figshare: doi:10.6084/m9.figshare.24138852 (Liu et al., 2023). All these data will be accessible upon publication.

Acknowledgements

We thank the researchers at all stations across the Qinghai-Tibetan Plateau for their work under the harsh climate and efforts to make their datasets publicly accessible. Their contributions regarding the establishment and maintenance of the eddy covariance and manipulative experiments made this study possible. We sincerely appreciate the editor and three reviewers for their contributions to the manuscript.

This work was financially supported by the Procurement Project of Qinghai Provincial Government “Evaluation of ecological environment comprehensive improvement in Muli mining area, Qinghai Province”

[2021046279], the Open Foundation of the Key Laboratory of Coupling Process and Effect of Natural Resources Elements [No. 2022KKTC006], and the National Key Scientific and Technological Infrastructure project “Earth System Numerical Simulation Facility” [2023-EL-PT-000433].

Appendix A. Supplementary data

Supplementary data to this article can be found online at <https://doi.org/10.1016/j.scitotenv.2024.170438>.

References

- Arndt, K.A., Lipson, D.A., Hashemi, J., Oechel, W.C., Zona, D., 2020. Snow melt stimulates ecosystem respiration in Arctic ecosystems. *Glob. Chang. Biol.* 26, 5042–5051. <https://doi.org/10.1111/gcb.15193>.
- Baldocchi, D., Falge, E., Gu, L., Olson, R., Hollinger, D., Running, S., Anthoni, P., Bernhofer, C., Davis, K., Evans, R., Fuentes, J., Goldstein, A., Katul, G., Law, B., Lee, X., Malhi, Y., Meyers, T., Munger, W., Oechel, W., Paw, K.T., Pilegaard, K., Schmid, H.P., Valentini, R., Verma, S., Vesala, T., Wilson, K., Wofsy, S., 2001. FLUXNET: a new tool to study the temporal and spatial variability of ecosystem-scale carbon dioxide, water vapor, and energy flux densities. *Bull. Am. Meteorol. Soc.* 82, 2415–2434. [https://doi.org/10.1175/1520-0477\(2001\)082<2415:FANTS>2.3.CO;2](https://doi.org/10.1175/1520-0477(2001)082<2415:FANTS>2.3.CO;2).
- Bao, T., Jia, G., Xu, X., 2021. Wetland heterogeneity determines methane emissions: a pan-arctic synthesis. *Environ. Sci. Technol.* 55, 10152–10163. doi:10.gnjvmk.
- Bibi, S., Wang, L., Li, X., Zhou, J., Chen, D., Yao, T., 2018. Climatic and associated cryospheric, biospheric, and hydrological changes on the Tibetan plateau: a review. *Int. J. Climatol.* 38, e1–e17. <https://doi.org/10.1002/joc.5411>.
- Biskaborn, B.K., Smith, S.L., Noetzli, J., Matthes, H., Vieira, G., Streletskev, D.A., Schoeneich, P., Romanovsky, V.E., Lewkowicz, A.G., Abramov, A., Allard, M., Boike, J., Cable, W.L., Christiansen, H.H., Delaloye, R., Diekmann, B., Drozdov, D., Etzelmüller, B., Grosse, G., Gugelmin, M., Ingeman-Nielsen, T., Isaksen, K., Ishikawa, M., Johansson, M., Johannsson, H., Joo, A., Kaverin, D., Khodolov, A., Konstantinov, P., Kröger, T., Lambiel, C., Lanckman, J.-P., Luo, D., Malkova, G., Meiklejohn, I., Moskalenko, N., Oliva, M., Phillips, M., Ramos, M., Sammel, A.B.K., Sergeev, D., Seybold, C., Skryabin, P., Vasilev, A., Wu, Q., Yoshikawa, K., Zheleznyak, M., Lantuit, H., 2019. Permafrost is warming at global scale. *Nat. Commun.* 10, 264. <https://doi.org/10.1038/s41467-018-08240-4>.
- Bodesheim, P., Jung, M., Gans, F., Mahecha, M.D., Reichstein, M., 2018. Upscaled diurnal cycles of land-atmosphere fluxes: a new global half-hourly data product. *Earth Syst. Sci. Data* 10, 1327–1365. <https://doi.org/10.5194/essd-10-1327-2018>.
- Bohn, T.J., Melton, J.R., Ito, A., Kleinen, T., Spaepen, R., Stocker, B.D., Zhang, B., Zhu, X., Schroeder, R., Glagolev, M.V., Maksyutov, S., Brovkin, V., Chen, G., Denisov, S.N., Eliseev, A.V., Gallego-Sala, A., McDonald, K.C., Rawlins, M.A., Riley, W.J., Subin, Z. M., Tian, H., Zhuang, Q., Kaplan, J.O., 2015. WETCHIMP-WSL: intercomparison of wetland methane emissions models over West Siberia. *Biogeosciences* 12, 3321–3349. <https://doi.org/10.5194/bg-12-3321-2015>.
- Breiman, L., 2001. Random forests. *Mach. Learn.* 45, 5–32. <https://doi.org/10.1023/A:1010933404324>.
- Brown, J., Ferrians, O., Heginbottom, J.A., Melnikov, E., 2002. Circum-arctic map of permafrost and ground-ice conditions. Version 2. Boulder, Colorado USA. NSIDC: National Snow and Ice Data Center. doi:10.7265/skbg-kf16.
- Chadburn, S.E., Aalto, T., Aurela, M., Baldocchi, D., Biasi, C., Boike, J., Burke, E.J., Comyn-Platt, E., Dolman, A.J., Duran-Rojas, C., Fan, Y., Friberg, T., Gao, Y., Gedney, N., Göckede, M., Hayman, G.D., Holl, D., Hugelius, G., Kutzbach, L., Lee, H., Lohila, A., Parmentier, F.-J.W., Sachs, T., Shurpali, N.J., Westermann, S., 2020. Modeled microbial dynamics explain the apparent temperature sensitivity of wetland methane emissions. *Global Biogeochem. Cycles* 34, e2020GB006678. <https://doi.org/10.1029/2020GB006678>.
- Chen, H., Zhu, Q., Peng, C., Wu, N., Wang, Y., Fang, X., Gao, Y., Zhu, D., Yang, G., Tian, J., Kang, X., Piao, S., Ouyang, H., Xiang, W., Luo, Z., Jiang, H., Song, X., Zhang, Y., Yu, G., Zhao, X., Gong, P., Yao, T., Wu, J., 2013. The impacts of climate change and human activities on biogeochemical cycles on the Qinghai-Tibetan plateau. *Glob. Chang. Biol.* 19, 2940–2955. <https://doi.org/10.1111/gcb.12277>.
- Chen, H., Liu, X., Xue, D., Zhu, D., Zhan, W., Li, W., Wu, N., Yang, G., 2021a. Methane emissions during different freezing-thawing periods from a fen on the Qinghai-Tibetan Plateau: four years of measurements. *Agric. For. Meteorol.* 297, 108279. <https://doi.org/10.1016/j.agrformet.2020.108279>.
- Chen, H., Xu, X., Fang, C., Li, B., Nie, M., 2021b. Differences in the temperature dependence of wetland CO₂ and CH₄ emissions vary with water table depth. *Nat. Clim. Chang.* 11, 766–771. <https://doi.org/10.1038/s41558-021-01108-4>.
- Chen, H., Ju, P., Zhu, Q., Xu, X., Wu, N., Gao, Y., Feng, X., Tian, J., Niu, S., Zhang, Y., Peng, C., Wang, Y., 2022. Carbon and nitrogen cycling on the Qinghai-Tibetan Plateau. *Nat. Rev. Earth Environ.* 3, 701–716. <https://doi.org/10.1038/s43017-022-00344-2>.
- Chen, L., Chen, Z., Jia, G., Zhou, J., Zhao, J., Zhang, Z., 2020. Influences of forest cover on soil freeze-thaw dynamics and greenhouse gas emissions through the regulation of snow regimes: a comparison study of the farmland and forest plantation. *Sci. Total Environ.* <https://doi.org/10.1016/j.scitotenv.2020.138403>.
- Chen, W., Zhang, F., Wang, B., Wang, J., Tian, D., Han, G., Wen, X., Yu, G., Niu, S., 2019. Diel and seasonal dynamics of ecosystem-scale methane flux and their determinants in an alpine meadow. *J. Geophys. Res. Biogeosci.* 124, 1731–1745. <https://doi.org/10.1029/2019JG005011>.
- Chen, X., Wang, G., Zhang, T., Mao, T., Wei, D., Song, C., Hu, Z., Huang, K., 2017. Effects of warming and nitrogen fertilization on GHG flux in an alpine swamp meadow of a permafrost region. *Sci. Total Environ.* 601–602, 1389–1399. <https://doi.org/10.1016/j.scitotenv.2017.06.028>.
- Conrad, R., 2007. Microbial ecology of methanogens and Methanotrophs. In: *Advances in Agronomy*, Academic Press. [https://doi.org/10.1016/S0065-2113\(07\)96005-8](https://doi.org/10.1016/S0065-2113(07)96005-8).
- Curry, C.L., 2007. Modeling the soil consumption of atmospheric methane at the global scale. *Global Biogeochem. Cycles* 21, GB4012. <https://doi.org/10.1029/2006GB002818>.
- Ito, A., Inatomi, M., 2012. Use of a process-based model for assessing the methane budgets of global terrestrial ecosystems and evaluation of uncertainty. *Biogeosciences* 9, 759–773. <https://doi.org/10.5194/bg-9-759-2012>.
- Jin, X.-Y., Jin, H., Iwahana, G., Marchenko, S.S., Luo, D., Li, X., Liang, S., 2021. Impacts of climate-induced permafrost degradation on vegetation: a review. *Adv. Clim. Chang. Res.* 12, 29–47. <https://doi.org/10.1016/j.accre.2020.07.002>.
- Kim, Y., Johnson, M.S., Knox, S.H., Black, T.A., Dalmagro, H.J., Kang, M., Kim, J., Baldocchi, D., 2020. Gap-filling approaches for eddy covariance methane fluxes: a comparison of three machine learning algorithms and a traditional method with principal component analysis. *Glob. Chang. Biol.* 26, 1499–1518. <https://doi.org/10.1111/geb.14845>.
- King, G., 1997. Responses of atmospheric methane consumption by soils to global climate change. *Glob. Chang. Biol.* 3, 351–362. <https://doi.org/10.1046/j.1365-2486.1997.00090.x>.
- Koskinen, M., Minkkinen, K., Ojanen, P., Kämäräinen, M., Laurila, T., Lohila, A., 2014. Measurements of CO₂ exchange with an automated chamber system throughout the year: challenges in measuring night-time respiration on porous peat soil. *Biogeosciences* 11, 347–363. <https://doi.org/10.5194/bg-11-347-2014>.
- Krzywinski, M., Altman, N., 2014. Visualizing samples with box plots. *Nat. Methods* 11, 119–120. <https://doi.org/10.1038/nmeth.2813>.
- Le Mer, J., Roger, P., 2001. Production, oxidation, emission and consumption of methane by soils: a review. *Eur. J. Soil Biol.* 37, 25–50. [https://doi.org/10.1016/S1164-5563\(01\)00676](https://doi.org/10.1016/S1164-5563(01)00676).
- Li, F., Yang, G., Peng, Y., Wang, G., Qin, S., Song, Y., Fang, K., Wang, J., Yu, J., Liu, L., Zhang, D., Chen, K., Zhou, G., Yang, Y., 2020a. Warming effects on methane fluxes differ between two alpine grasslands with contrasting soil water status. *Agric. For. Meteorol.* 290, 107988. <https://doi.org/10.1016/j.agrformet.2020.107988>.
- Li, H., Zhu, J., Zhang, F., Qin, G., Yang, Y., Li, Y., Wang, J., Cao, G., Li, Y., Zhou, H., Du, M., 2022. The predominance of nongrowing season emissions to the annual methane budget of a semiarid alpine meadow on the northeastern Qinghai-Tibetan plateau. *Ecosystems* 25, 526–536. <https://doi.org/10.1007/s10021-021-00669-x>.
- Li, J., Pei, J., Fang, C., Li, B., Nie, M., 2023a. Opposing seasonal temperature dependencies of CO₂ and CH₄ emissions from wetlands. *Glob. Chang. Biol.* 29, 1133–1143. <https://doi.org/10.1111/gcb.16528>.
- Li, R., Zhang, M., Andreeva, V., Pei, W., Zhou, Y., Misailov, I., Basharin, N., 2023b. Impact of climate warming on permafrost changes in the Qinghai-Tibet plateau. *Cold Reg. Sci. Technol.* 205, 103692. <https://doi.org/10.1016/j.coldregions.2022.103692>.
- Li, T., Lu, Y., Yu, L., Sun, W., Zhang, Q., Zhang, W., Wang, G., Qin, Z., Yu, L., Li, H., Zhang, R., 2020b. Evaluation of CH4MOD_{wetland} and terrestrial ecosystem model (TEM) used to estimate global CH₄ emissions from natural wetlands. *Geosci. Model Dev.* 13, 3769–3788. <https://doi.org/10.5194/gmd-13-3769-2020>.
- Liu, Z., Chen, B., Wang, S., Xu, X., Chen, J., Wang, X., Zheng, C., Zhu, K., Wang, X., 2023. Collected observations of CH₄ fluxes in the QTP. doi:<https://doi.org/10.6084/m9.figshare.24138852.v2> (2023/9/14).
- Long, K.D., Flanagan, L.B., Cai, T., 2010. Diurnal and seasonal variation in methane emissions in a northern Canadian peatland measured by eddy covariance. *Glob. Chang. Biol.* 16, 2420–2435. <https://doi.org/10.1111/j.1365-2486.2009.02083.x>.
- Peng, H., Guo, Q., Ding, H., Hong, B., Zhu, Y., Hong, Y., Cai, C., Wang, Y., Yuan, L., 2019. Multi-scale temporal variation in methane emission from an alpine peatland on the eastern Qinghai-Tibetan plateau and associated environmental controls. *Agric. For. Meteorol.* 276–277, 107616. <https://doi.org/10.1016/j.agrformet.2019.107616>.
- Qin, X., Haiming, W., Jian, L., 2014. Methane emissions from wetlands in China: effects of wetland type and climate zone. *Carb. Manag.* 5, 535–541. <https://doi.org/10.1080/17583004.2015.1040947>.
- Ran, Y., Li, X., Cheng, G., 2018. Climate warming over the past half century has led to thermal degradation of permafrost on the Qinghai-Tibet Plateau. *Cryosphere* 12, 595–608. <https://doi.org/10.5194/tc-12-595-2018>.
- Richardson, A.D., Hollinger, D.Y., Burba, G.G., Davis, K.J., Flanagan, L.B., Katul, G.G., William Munger, J., Ricciuto, D.M., Stoy, P.C., Suyker, A.E., Verma, S.B., Wofsy, S.C., 2006. A multi-site analysis of random error in tower-based measurements of carbon and energy fluxes. *Agric. For. Meteorol.* 136, 1–18. <https://doi.org/10.1016/j.agrformet.2006.01.007>.
- Running, S., Mu, Q., Zhao, M., 2021. MODIS/Terra Net Evapotranspiration 8-Day L4 Global 500m SIN Grid V061. doi:<https://doi.org/10.5067/MODIS/MOD16A2.061> (2023/11/27).
- Salmon, E., Jégou, F., Guenet, B., Jourdain, L., Qiu, C., Bastrikov, V., Guimbaud, C., Zhu, D., Ciais, P., Peylin, P., Gogo, S., Laggoun-Défarge, F., Aurela, M., Bret-Harte, M.S., Chen, J., Chojnicki, B.H., Chu, H., Edgar, C.W., Euskirchen, E.S., Flanagan, L.B., Fortuniak, K., Holl, D., Klatt, J., Kolle, O., Kowalska, N., Kutzbach, L., Lohila, A., Merbold, L., Pawlak, W., Sachs, T., Ziemblińska, K., 2022. Assessing methane emissions for northern peatlands on ORCHIDEE-PEAT revision 7020. *Geosci. Model Dev.* 15, 2813–2838. <https://doi.org/10.5194/gmd-15-2813-2022>.
- Saunois, M., Stavert, A.R., Poulter, B., Bousquet, P., Canadell, J.G., Jackson, R.B., Raymond, P.A., Slagsgokkenky, E.J., Houweling, S., Patra, P.K., Ciais, P., Arora, V.K.,

- Bastviken, D., Bergamaschi, P., Blake, D.R., Brailsford, G., Bruhwiler, L., Carlson, K.M., Carroll, M., Castaldi, S., Chandra, N., Crevoisier, C., Crill, P.M., Covey, K., Curry, C.L., Etiope, G., Frankenberger, C., Gedney, N., Hegglin, M.I., Höglund-Isaksson, L., Hugelius, G., Ishizawa, M., Ito, A., Janssens-Maenhout, G., Jensen, K.M., Joos, F., Kleinen, T., Krummel, P.B., Langenfelds, R.L., Laruelle, G.G., Liu, L., Machida, T., Maksyutov, S., McDonald, K.C., McNorton, J., Miller, P.A., Melton, J.R., Morino, I., Müller, J., Murguia-Flores, F., Naik, V., Niwa, Y., Noce, S., O'Doherty, S., Parker, R.J., Peng, C., Peng, S., Peters, G.P., Prigent, C., Prinn, R., Ramonet, M., Regnier, P., Riley, W.J., Rosentreter, J.A., Segers, A., Simpson, I.J., Shi, H., Smith, S.J., Steele, L.P., Thornton, B.F., Tian, H., Tohjima, Y., Tubiello, F.N., Tsuruta, A., Viovy, N., Voulgarakis, A., Weber, T.S., Van Weele, M., Van Der Werf, G.R., Weiss, R.F., Worthy, D., Wunch, D., Yin, Y., Yoshida, Y., Zhang, W., Zhang, Z., Zhao, Y., Zheng, B., Zhu, Q., Zhu, Q., Zhuang, Q., 2020. The global methane budget 2000–2017. *Earth Syst. Sci. Data* 12, 1561–1623. <https://doi.org/10.5194/essd-12-1561-2020>.
- Segers, R., 1998. Methane production and methane consumption: a review of processes underlying wetland methane fluxes. *Biogeochemistry* 41, 23–51. <https://doi.org/10.1023/A:1005929032764>.
- Shindell, D.T., Faluvegi, G., Koch, D.M., Schmidt, G.A., Unger, N., Bauer, S.E., 2009. Improved attribution of climate forcing to emissions. *Science* 326, 716–718. <https://doi.org/10.1126/science.1174760>.
- Song, C., Xu, X., Tian, H., Wang, Y., 2009. Ecosystem–atmosphere exchange of CH₄ and N₂O and ecosystem respiration in wetlands in the Sanjiang Plain. *Northeastern China. Glob. Change Biol.* 15, 692–705. <https://doi.org/10.1111/j.1365-2486.2008.01821.x>.
- Song, W., Wang, H., Wang, G., Chen, L., Jin, Z., Zhuang, Q., He, J., 2015. Methane emissions from an alpine wetland on the Tibetan plateau: neglected but vital contribution of the nongrowing season. *J. Geophys. Res. Biogeosci.* 120, 1475–1490. <https://doi.org/10.1002/2015JG003043>.
- Treat, C.C., Bloom, A.A., Marushchak, M.E., 2018. Nongrowing season methane emissions—a significant component of annual emissions across northern ecosystems. *Glob. Chang. Biol.* 24, 3331–3343. <https://doi.org/10.1111/gcb.14137>.
- Wang, J., Luo, Y., Quan, Q., Ma, F., Tian, D., Chen, W., Wang, S., Yang, L., Meng, C., Niu, S., 2021. Effects of warming and clipping on CH₄ and N₂O fluxes in an alpine meadow. *Agric. For. Meteorol.* 297, 108278 <https://doi.org/10.1016/j.agrformet.2020.108278>.
- Wang, P., Wang, J., Elberling, B., Yang, L., Chen, W., Song, L., Yan, Y., Wang, S., Pan, J., He, Y., Niu, S., 2022. Increased annual methane uptake driven by warmer winters in an alpine meadow. *Glob. Chang. Biol.* 28, 3246–3259. <https://doi.org/10.1111/gcb.16120>.
- Wang, X., Wang, S., Li, X., Chen, B., Wang, J., Huang, M., Rahman, A., 2020a. Modelling rice yield with temperature optima of rice productivity derived from satellite NIRv in tropical monsoon area. *Agric. For. Meteorol.* 294, 108135 <https://doi.org/10.1016/j.agrformet.2020.108135>.
- Wang, Y., Chen, H., Zhu, Q., Peng, C., Wu, N., Yang, G., Zhu, D., Tian, J., Tian, L., Kang, X., He, Y., Gao, Y., Zhao, X., 2014. Soil methane uptake by grasslands and forests in China. *Soil Biol. Biochem.* 74, 70–81. <https://doi.org/10.1016/j.soilbio.2014.02.023>.
- Wang, Z., Wu, J., Niu, B., He, Y., Zu, J., Li, M., Zhang, X., 2020b. Vegetation expansion on the Tibetan plateau and its relationship with climate change. *Remote Sens.* 12, 4150. <https://doi.org/10.3390/rs12244150>.
- Watts, J.D., Farina, M., Kimball, J.S., Schiferl, L.D., Liu, Z., Arndt, K.A., Zona, D., Ballantyne, A., Euskirchen, E.S., Parmentier, F.-J.W., Helbig, M., Sonnentag, O., Tagesson, T., Rinne, J., Ikawa, H., Ueyama, M., Kobayashi, H., Sachs, T., Nadeau, D.F., Kochendorfer, J., Jackowicz-Korczynski, M., Virkala, A., Aurela, M., Commane, R., Byrne, B., Birch, L., Johnson, M.S., Madani, N., Rogers, B., Du, J., Endsley, A., Savage, K., Poultier, B., Zhang, Z., Bruhwiler, L.M., Miller, C.E., Goetz, S., Oechel, W.C., 2023. Carbon uptake in Eurasian boreal forests dominates the high-latitude net ecosystem carbon budget. *Glob. Chang. Biol.* 29, 1870–1889. <https://doi.org/10.1111/geb.16553>.
- Wei, D., Wang, X., 2017. Recent climatic changes and wetland expansion turned Tibet into a net CH₄ source. *Clim. Chang.* 144, 657–670. <https://doi.org/10.1007/s10584-017-2069-y>.
- Wei, D., Ri, X., Tarchen, T., Wang, Y., Wang, Y., 2015. Considerable methane uptake by alpine grasslands despite the cold climate: in situ measurements on the central Tibetan plateau, 2008–2013. *Glob. Chang. Biol.* 21, 777–788. <https://doi.org/10.1111/gcb.12690>.
- Wille, C., Kutzbach, L., Sachs, T., Wagner, D., Pfeiffer, E.M., 2008. Methane emission from Siberian arctic polygonal tundra: eddy covariance measurements and modeling. *Glob. Chang. Biol.* 14, 1395–1408. <https://doi.org/10.1111/j.1365-2486.2008.01586.x>.
- Wu, F., Cao, S., Cao, G., Chen, K., Peng, C., 2021. The characteristics and seasonal variation of methane fluxes from an alpine wetland in the Qinghai lake watershed. *China. Wetlands* 41, 53. <https://doi.org/10.1007/s13157-021-01415-8>.
- Wu, Q., Zhang, T., 2008. Recent permafrost warming on the Qinghai-Tibetan plateau. *J. Geophys. Res.-Atmos.* 113 <https://doi.org/10.1029/2007JD009539>.
- Yang, M., Nelson, F.E., Shiklomanov, N.I., Guo, D., Wan, G., 2010. Permafrost degradation and its environmental effects on the Tibetan Plateau: a review of recent research. *Earth Sci. Rev.* 103, 31–44. <https://doi.org/10.1016/j.earscirev.2010.07.002>.
- Yao, Z., Ma, L., Zhang, H., Zheng, X., Wang, K., Zhu, B., Wang, R., Wang, Y., Zhang, W., Liu, C., Butterbach-Bahl, K., 2019. Characteristics of annual greenhouse gas flux and NO release from alpine meadow and forest on the eastern Tibetan plateau. *Agric. For. Meteorol.* 272–273, 166–175. <https://doi.org/10.1016/j.agrformet.2019.04.007>.
- Yu, L., Wang, H., Wang, G., Song, W., Huang, Y., Li, S.-G., Liang, N., Tang, Y., He, J.-S., 2013. A comparison of methane emission measurements using eddy covariance and manual and automated chamber-based techniques in Tibetan plateau alpine wetland. *Environ. Pollut.* 181, 81–90. <https://doi.org/10.1016/j.envpol.2013.06.018>.
- Yu, L., Huang, Y., Zhang, W., Li, T., Sun, W., 2017. Methane uptake in global forest and grassland soils from 1981 to 2010. *Sci. Total Environ.* 607–608, 1163–1172. <https://doi.org/10.1016/j.scitotenv.2017.07.082>.
- Yvon-Durocher, G., Allen, A.P., Bastviken, D., Conrad, R., Gudasz, C., St-Pierre, A., Thanh-Duc, N., del Giorgio, P.A., 2014. Methane fluxes show consistent temperature dependence across microbial to ecosystem scales. *Nature* 507, 488–491. <https://doi.org/10.1038/nature13164>.
- Zhang, H., Yao, Z., Ma, L., Zheng, X., Wang, R., Wang, K., Liu, C., Zhang, W., Zhu, B., Tang, X., Hu, Z., Han, S., 2019. Annual methane emissions from degraded alpine wetlands in the eastern Tibetan plateau. *Sci. Total Environ.* 657, 1323–1333. <https://doi.org/10.1016/j.scitotenv.2018.11.443>.
- Zhang, J., Zhu, Q., Yuan, M., Liu, X., Chen, H., Peng, C., Wang, M., Yang, Z., Jiang, L., Zhao, P., 2020a. Extrapolation and uncertainty evaluation of carbon dioxide and methane emissions in the Qinghai-Tibetan plateau wetlands since the 1960s. *Front. Earth Sci.* 8, 361. <https://doi.org/10.3389/feart.2020.00361>.
- Zhang, S., Zhang, F., Shi, Z., Qin, A., Wang, H., Sun, Z., Yang, Z., Zhu, Y., Pang, S., Wang, P., 2020b. Sources of seasonal wetland methane emissions in permafrost regions of the Qinghai-Tibet plateau. *Sci. Rep.* 10, 7520. <https://doi.org/10.1038/s41598-020-63054-z>.
- Zhang, S., Ma, J., Zhang, X., Guo, C., 2023. Atmospheric remote sensing for anthropogenic methane emissions: applications and research opportunities. *Sci. Total Environ.* 893, 164701 <https://doi.org/10.1016/j.scitotenv.2023.164701>.
- Zhang, Z., Wang, G., Wang, H., Qi, Q., Yang, Y., He, J., 2021. Warming and drought increase but wetness reduces the net sink of CH₄ in alpine meadow on the Tibetan plateau. *Appl. Soil Ecol.* 167, 104061 <https://doi.org/10.1016/j.apsoil.2021.104061>.
- Zhao, Z., Zhang, Y., 2015. Recent changes in wetlands on the Tibetan plateau: a review. *J. Geogr. Sci.* 25, 879–896. <https://doi.org/10.1007/s11442-015-1208-5>.
- Zheng, Y., Yang, W., Sun, X., Wang, S., Rui, Y., Luo, C., Guo, L., 2012. Methanotrophic community structure and activity under warming and grazing of alpine meadow on the Tibetan plateau. *Appl. Microbiol. Biotechnol.* 93, 2193–2203. <https://doi.org/10.1007/s00253-011-3535-5>.
- Zhou, G., Ren, H., Liu, T., Zhou, L., Ji, Y., Song, X., Lv, X., 2023. A new regional vegetation mapping method based on terrain-climate-remote sensing and its application on the Qinghai-Xizang plateau. *Sci. China Earth Sci.* 66, 237–246. <https://doi.org/10.1007/s11430-022-1006-1>.
- Zhuang, Q., Chen, M., Xu, K., Tang, J., Saikawa, E., Lu, Y., Melillo, J.M., Prinn, R.G., McGuire, A.D., 2013. Response of global soil consumption of atmospheric methane to changes in atmospheric climate and nitrogen deposition. *Global Biogeochem. Cycles* 27, 650–663. <https://doi.org/10.1002/gbc.20057>.
- Zona, D., Gioli, B., Commane, R., Lindaas, J., Wofsy, S.C., Miller, C.E., Dinardo, S.J., Dengel, S., Sweeney, C., Karion, A., Chang, R.Y.W., Henderson, J.M., Murphy, P.C., Goodrich, J.P., Moreaux, V., Liljedahl, A., Watts, J.D., Kimball, J.S., Lipson, D.A., Oechel, W.C., 2016. Cold season emissions dominate the Arctic tundra methane budget. *Proc. Natl. Acad. Sci. U. S. A.* 113, 40–45. <https://doi.org/10.1073/pnas.1516017113>.